APPLICATIONS OF
MODELLING AND SIMULATION
http://arqiipubl.com/ams eISSN 2600-8084 VOL 6, 2022, 150-157

Modeling and Performance Analysis of an In-wheel Permanent Magnet Brushless DC (PM BLDC) Motor in MATLAB

Basant Ale

Department of Mechanical Engineering, Pulchowk Campus (IOE), Tribhuvan University, Lalitpur, Nepal

Corresponding author: basant.070bme612@pcampus.edu.np

Submitted 24 November 2022, Revised 29 December 2022, Accepted 30 December 2022, Available online 31 December 2022.

Abstract: The electric traction motor is modeled and simulated to develop design parameters, analyze the motor performances, study the motor application, and other various reasons. The mathematical modeling of a traction motor requires governing equations with several physical parameters that depend upon the motor's construction parameters. It is challenging to get the motor's mechanical and electrical parameters for modeling and simulation. In this paper, a simple in-wheel PM BLDC motor is developed in MATLAB software. The motor's performance analysis is executed for different speed profiles and torque-speed operating points are studied. The torque-speed envelope of an actual 1.5 kW rated power in-wheel BLDC motor is compared with the data generated from the simulation. The proposed model is expected to be helpful in the selection of PM BLDC motors at the design stage for Electric Vehicle applications.

Keywords: Electric vehicle; Electric motor drives; Longitudinal vehicle dynamics; PM BLDC motor.

1. INTRODUCTION

Electric Drive is important sub system of any Electric Vehicle (EV) system. It usually comprises one or more traction motors and the associated power electronics and controls. Most general traction motors used in EVs are DC motors (DC), Induction motors (IM), Permanent Magnet Synchronous motors (PMSM) and Switched Reluctance motors (SRM). Among various types of motor drives, permanent magnet (PM) brushless motor drives are becoming dominant in the market, mainly because of comparatively high-power density and high efficiency [1-3]. Low-powered EVs like electric scooters mostly use in-wheel motors. Such motors demand a high torque-to-weight ratio, a high torque-to-volume ratio, a simple mechanical design, low weight, and high efficiency. Because of these features, electric vehicles with gearless propulsion systems use Permanent Magnet Brushless DC (PM BLDC) motors [4-6].

In propulsion applications, the motor operates over its entire torque-speed range. Therefore, it must be studied at all possible torque/speed combinations within the motor operating envelope [7]. Generally, the mathematical modeling of a traction motor requires governing equations with several physical parameters that depend upon the motor's construction parameters [8, 9]. It is not easy to obtain their mechanical and electrical parameter values. A method to determine parameters for motor modeling based on vehicle performances has been developed [10]. However, if objective of modeling is to select a suitable motor for an application, then the above methods are time-consuming and quite complex. In this paper, a general BLDC motor with vehicle dynamics is developed to generate a torque-versus-speed profile under different driving conditions. The generated torque-speed values of the motor are compared with an actual in-wheel PM BLDC motor's operating region.

This paper is mainly composed of five sections. The principle working mechanism of the PM BLDC motor is explained briefly with governing equations in Section 2. Section 3 covers development of a PM BLDC motor model in MATLAB considering design parameters. Longitudinal vehicle force dynamics, 3-phase Inverter, rotor position sensor, gate signal generator, controllers, and sensor subsystems are also modeled and explained. Section 4 includes simulation results, data comparisons, and visualizations. It explains why the model is suitable to use at the design stage for selecting BLDC motor for EV applications. The last section ends with the conclusion of the study.

2. OVERVIEW OF PERMANENT MAGNET BRUSHLESS DC MOTOR

2.1 Structure of PM BLDC

The PM BLDC motor has 3-phase stator windings and a PM rotor. The key feature of PM BLDC is to use electronic commutation in place of mechanical commutation. PM BLDC motor is designed with the trapezoidal distribution of air-gap flux and concentrated arrangement of stator windings. The motor speed control is simple, in which the stator currents are controlled in such a way that the rectangular current properly aligns with the trapezoidal flux [1, 11].

2.2 Position Sensor

The position sensors, like the Hall sensor, installed in the motor can detect the rotor position and transform it into an electrical signal, providing the correct commutation information for the logic switch circuit [12]. The commutation logic is added to the model to dynamically change the switching pattern for continuous rotation of the motor.

2.3 Drive Mode

Generally, for wye-wound BLDC motors, a full bridge driving circuit is used. The power switches are used to turn on or off the currents of the windings according to the logic signals produced by Hall sensors. The two-phase conduction mode is implemented in this model. The conduction order and instant are determined by the rotor position information. The bridge converter commutates once the rotor rotates at a 60° electrical angle, and the magnetic status is consequently changed. There are six magnetic sectors and two-phase windings are conducted in each sector. The current flowing continuously in each winding results in torque, which has a time of 120° electric angles [12].

2.4 Mathematical Equations of PM BLDC Motor

The motor is assumed to be a 3-phase star-connected stator circuit. Since the flux linkage is trapezoidal, it is necessary to derive the model of the PM brushless machine in terms of its state variables [1]. Due to a smooth cylindrical rotor, there is no rotor inductance with angle, and assuming three identical p hase, the self and mutual inductance L and M of the three phases are equal. The motor has stator resistance of R_s. The stator currents i_a, i_b and i_c are restricted to be balanced and it can be described by the following voltage equations [13].

$$V_a = i_a R_s + (L - M)\frac{d}{dt} i_a + e_a \quad (1)$$

$$V_b = i_b R_s + (L - M)\frac{d}{dt} i_b + e_b \quad (2)$$

$$V_c = i_c R_s + (L - M)\frac{d}{dt} i_c + e_c \quad (3)$$

Where e_a, e_b and e_c are the induced back emf. Equations (1), (2) and (3) lead to PM BLDC Motor model as:

$$\begin{bmatrix} V_a \\ V_b \\ V_c \end{bmatrix} = R_s \begin{bmatrix} 1 & 0 & 0 \\ 0 & 1 & 0 \\ 0 & 0 & 1 \end{bmatrix} \begin{bmatrix} i_a \\ i_b \\ i_c \end{bmatrix} + (L - M) \begin{bmatrix} 1 & 0 & 0 \\ 0 & 1 & 0 \\ 0 & 0 & 1 \end{bmatrix} \frac{d}{dt} \begin{bmatrix} i_a \\ i_b \\ i_c \end{bmatrix} + \begin{bmatrix} e_a \\ e_b \\ e_c \end{bmatrix} \quad (4)$$

The total electromagnetic torque T_e with respect to rotor rotational speed w_r is given by:

$$T_e = (e_a i_a + e_b i_b + e_c i_c)/w_r \quad (5)$$

The total electromagnetic torque in terms of rotor position θ_r, peak mutual flux linkage of stator winding λ_p and waveform function f of back emf of each phase is given as:

$$T_e = \lambda_p (f_a(\theta_r) i_a + f_b(\theta_r) i_b + f_c(\theta_r) i_c) \quad (6)$$

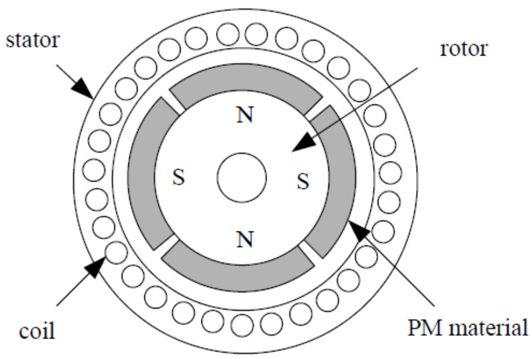

Figure 1. Cross section of a 4-pole PM BLDC motor [12]

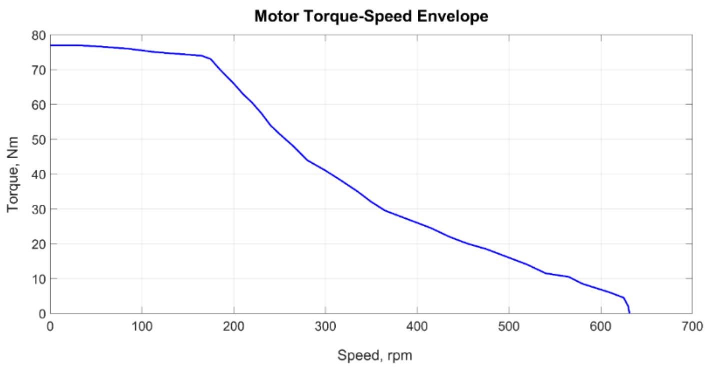

Figure 2. Torque vs Speed envelope of the reference motor (Source: https://evnepalmotors.com/)

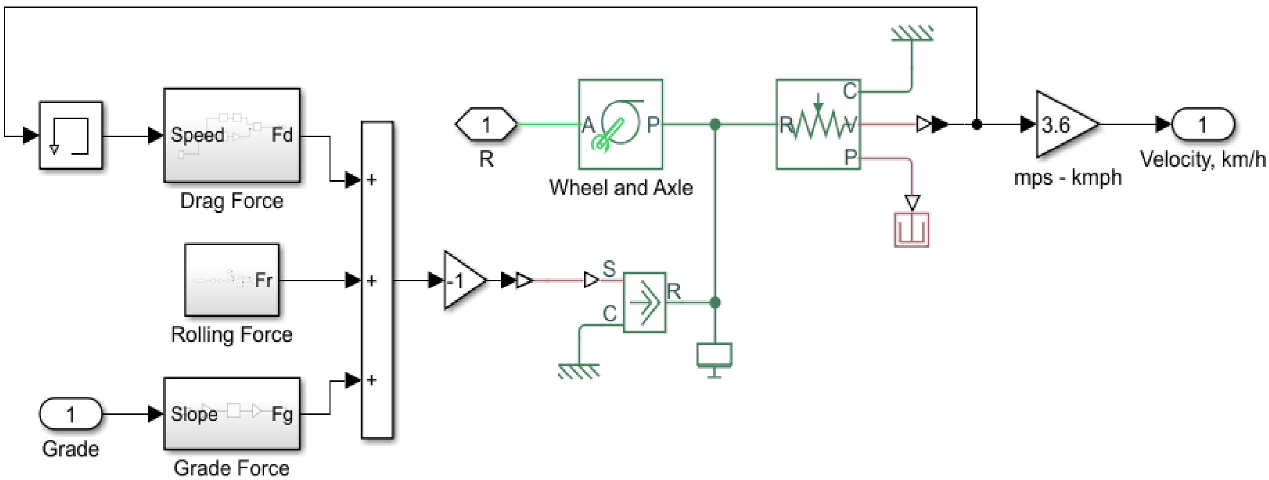

Figure 3. Longitudinal vehicle dynamics model of the vehicle

2.5 Reference Motor's Torque-Speed Profile

In this paper, a 1.5 kW in-wheel motor with the torque-speed operating region as in Figure 2 is selected for the model analysis and verification purpose. The objective of this paper is to study the sizing of the motor for an electric scooter at the design stage. The simulation of the motor model for different speed profiles gives the torque-speed operating points, which are compared with the manufacturer's data. The comparison results are used to study the vehicle performance and determine the motor specifications.

3. MODEL DEVELOPMENT IN MATLAB

3.1 Profile Longitudinal Vehicle Dynamics Model

Vehicle dynamics of a lightweight e-scooter are assumed here for modeling and simulation purposes. The longitudinal dynamic model of the vehicle is shown in Figure 3. The scooter is rear-wheel-driven. The backward method or the effect-cause method is adopted in this model [14]. During driving, several resistance forces act on the vehicle and the traction motor must provide enough force on the wheel to propel the vehicle. The traction force of a vehicle F_{track} is the sum of gradient force F_{grade} rolling resistance force F_{roll}, drag force F_{drag} and inertial force $F_{inertia}$ as given by the following equations [15]:

$$F_{tract} = F_{inertia} + F_{grade} + F_{roll} + F_{drag} \quad (7)$$

$$F_{tract} = m\frac{dv}{dt} + mg\sin(\alpha) + sign(v)mg\cos(\alpha)C_r + sign(v+v_w)\frac{1}{2}\rho_{air}C_d A_f (v+v_w)^2$$

$$C_r = 0.01\left(1 + \frac{3.6}{100}v\right) \quad (8)$$

m is the mass of the vehicle and rider, *g* is the acceleration due to gravity, v is the vehicle's speed, α is the road slope in radian, C_r is the tire rolling resistance coefficient, v_w is the headwind speed, ρ_{air} is the density of air at 20°C, C_d is the aerodynamic drag coefficient, and A_f is the frontal area of the vehicle. For the calculation purpose, the value of m is 150 kg, g is 9.81 m/s^2, C_d is 0.88 [18], ρ_{air} 1.225 kg/m^3, and A_f is 0.614 m^2. The rear wheel size is '90/90-12'.

Gearless in-wheel motor has transmission ratio equals to 1. Hence, traction torque τ_w acting on the wheel of radius r_w and motor power *P* can be obtained as:

$$\tau_w = F_{tract} r_w \tag{9}$$
$$P = F_{tract} v \tag{10}$$

3.2 PM BLDC Motor Model

The MATLAB-Simscape block called 'Brushless DC Motor' is used in this model to represent a wye-wound 3-phase PM BLDC motor with a trapezoidal back EMF profile. The rotor angle is selected to be 120° per number of pole pairs over which the back emf is constant. All other parameters are set by default. The inputs of the block, phase a, b, and c receive a controlled voltage supply from the drive system.

3.3 Hall Sensor and Commutation Logic Model

The ideal rotational motion sensor block is used to determine the rotor position. The hall sensor model uses the information of rotor position to compute the current sector. The conduction order and instant are determined by the rotor position information. The two-phase 120º conduction scheme is adopted as the switching method. In this scheme, at any instant, only two phases are conducted with the conduction interval of 120º while the remaining phase is non-conductive. For normal operation, the phase current waveform is near rectangular in shape and easily reaches the current demand. The corresponding switching sequence is summarized in Table 1 [1]. As per the sector position, the commutation logic selects the above switching patterns which are fed to the 3-phase inverter (Figure 4), and hence the motor is energized.

3.4 PI Controller Model

The detailed design of a control algorithm for the motor speed controller [16, 17] is beyond the scope of this paper. A simple PI controller has been used to regulate the speed in this model. Reference speed and vehicle's actual speed are input to the PI controller which generates a reference value of the controlled voltage supply to the inverter system. For a PI controller, one tuning method is to set the integral part to zero first, then increase the proportional part until the system response is stable. Finally, tune the integral part to improve the dynamic response ability and static stability [12]. The MATLAB Simulink's inbuilt PID tuner toolbox is used to fine tune the controller to get least deviation between the reference and actual vehicle speed. Hence, Proportional gain K_p and Integral gain K_i of the PI controller are obtained to be 1000 and 0.01 respectively.

Table 1. Commutation logic

Rotor position	Sector position	AH AL BH BL CH CL (Switch pattern)
$0° < \theta_r < 60°$	Sector 1	1 0 0 0 0 1
$60° < \theta_r < 120°$	Sector 2	0 0 1 0 0 1
$120° < \theta_r < 180°$	Sector 3	0 1 1 0 0 0
$180° < \theta_r < 240°$	Sector 4	0 1 0 0 1 0
$240° < \theta_r < 300°$	Sector 5	0 0 0 1 1 0
$300° < \theta_r < 360°$	Sector 6	1 0 0 1 0 0

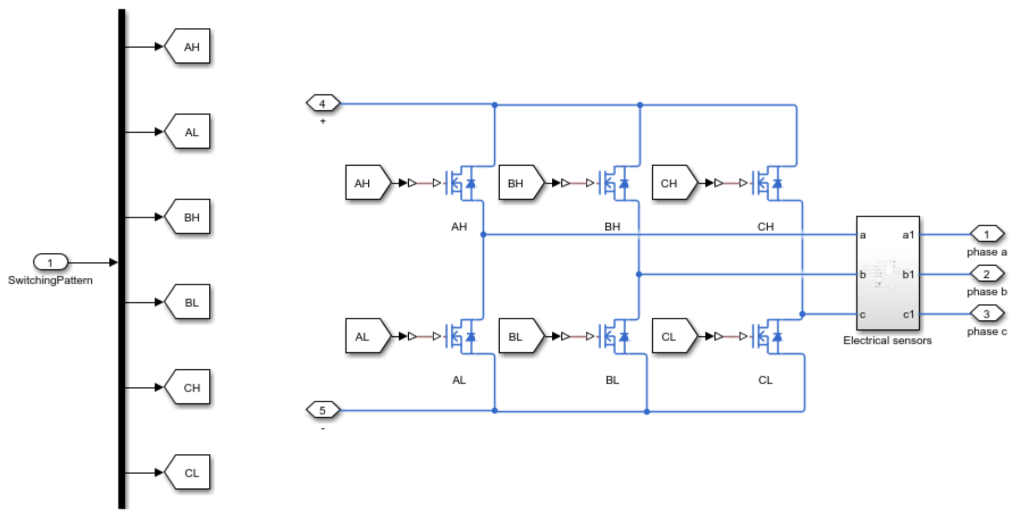

Figure 4. Three phase inverter model

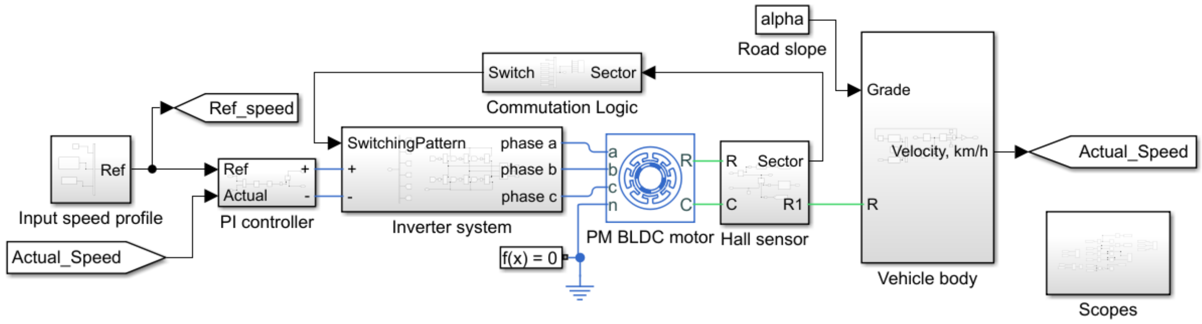

Figure 5. The overall model

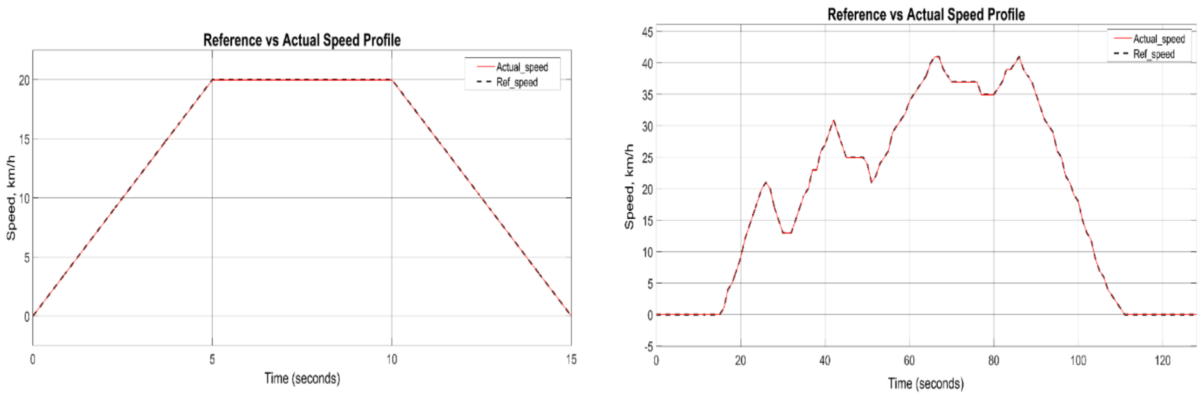

Figure 6. Speed tracking of Case 1 and Case 2 speed profiles

This model contains speed profiles that represent vehicle driving behavior. The speed value, in km/h, is fed to the PI Controller as input. Two cases of speed profiles are used as follows:

- Case 1: Trapezoidal signal is used to represent starting acceleration behavior of the vehicle. 20 km/h speed is targeted to achieve in 5 seconds i.e., 1.11 m/s^2 acceleration at the start.
- Case 2: Indian Drive Cycle (IDC) is used to represent high speed and high acceleration driving behavior. The cycle represents a 0.7 km route, an average speed of 19 km/h, a maximum speed of 42 km/h, and a duration of 128 seconds.

The final model is obtained after integrating above models is shown in Figure 5.

4. SIMULATION RESULTS AND DISCUSSION

The maximum speed error values (difference between reference and actual speed profiles) of Case 1 and Case 2 are 0.03 and 0.06, respectively. Figure 6 confirms that the PI Speed controller used in the model is working well. Figure 7 shows the square waveform of the current and trapezoidal waveform of voltage of phase *A* of the PM BLDC motor model for Case 1. Torque ripples present in the waveforms could be smoothed out; however, it is not in the scope of this paper.

According to the defined switching patterns, pulses were generated in switches 1-6 of the three-phase inverter for Case 1 as shown in Figure 8. Figures 9 and 10 show the torque, speed, and power demand graph for speed profile Case 1 and Case 2, respectively, when the vehicle model is simulated on road with slope $\alpha = 0°$. In Case 1, the vehicle needed a peak torque of 31 Nm, demanding 1.1 kW peak power, to accelerate from rest to 20 km/h in 5 seconds. In Case 2, a peak torque of 26 Nm is needed to achieve the peak speed of 42 km/h during a 128-second drive cycle, demanding 1.5 kW peak power.

Furthermore, the simulated operating points of Case 1 and Case 2 were plotted on the torque-speed Region of the actual motor. From Figure 11, it is observed that the operating points of Case 1 scattered inside the motor's torque-speed envelope. This means the vehicle is able to achieve acceleration as per the Case 1 speed profile. Further simulation showed that the Case 1 operating points were under the T-N envelope for road slope $\alpha < 5°$. However, some of the operating points of Case 2 scattered out of the motor's torque-speed envelope. Hence, it is concluded that the motor is unable to achieve higher speeds under the given load.

A modified IDC drive cycle is used for another simulation where the maximum vehicle speed is limited to 25 km/h. In Figure 12, it is observed that the motor's torque-speed envelope included most of the operating points of the modified Case 2 speed profile. It is noted that the operating points are below the lower half portion of the torque region. This shows that the motor is not efficient at exploiting its full torque capacity. Similar simulations were done for different vehicle input parameters like vehicle mass, road slope, drive wheel size, etc. After many simulations, it is concluded that the selected motor is only suitable for low-speed applications and is not capable of propelling the designed scooter in Indian Drive Cycle velocity profile.

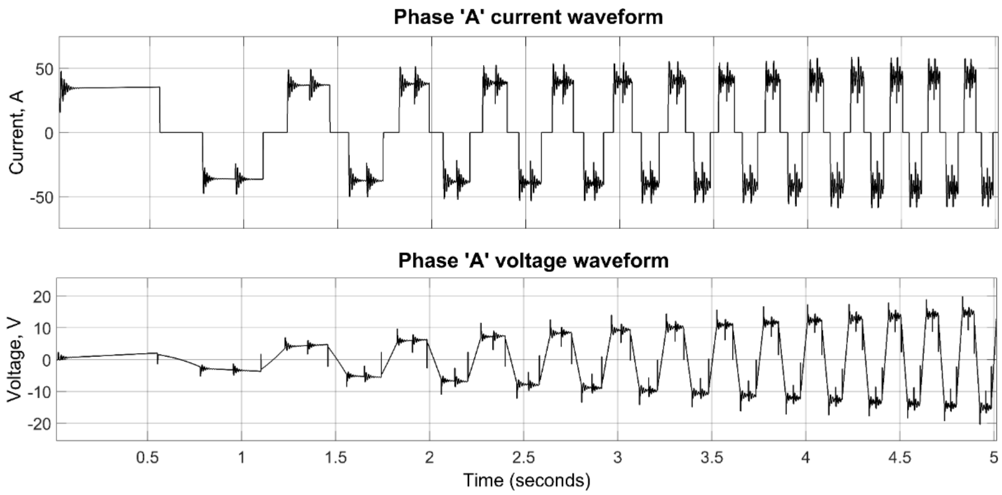

Figure 7. Current and voltage waveform of phase A of motor

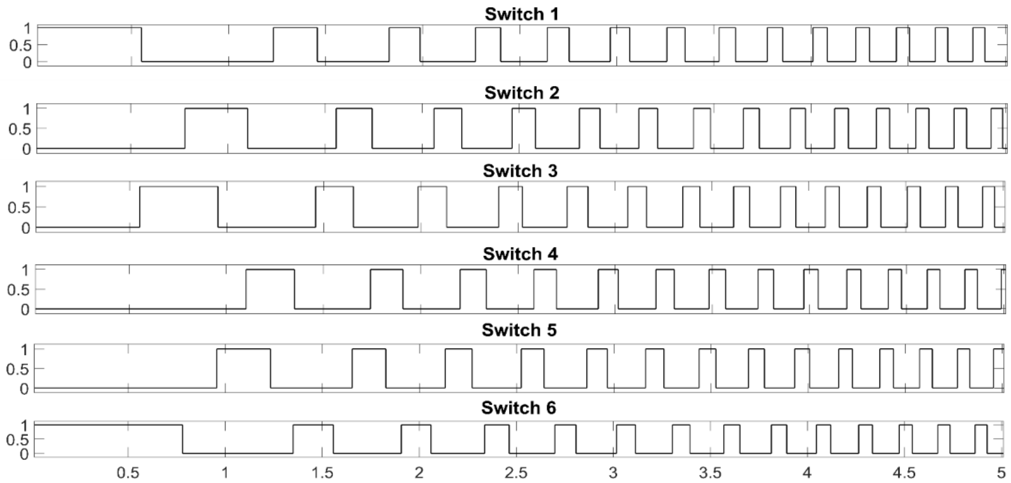

Figure 8. Pulses generated in the switches

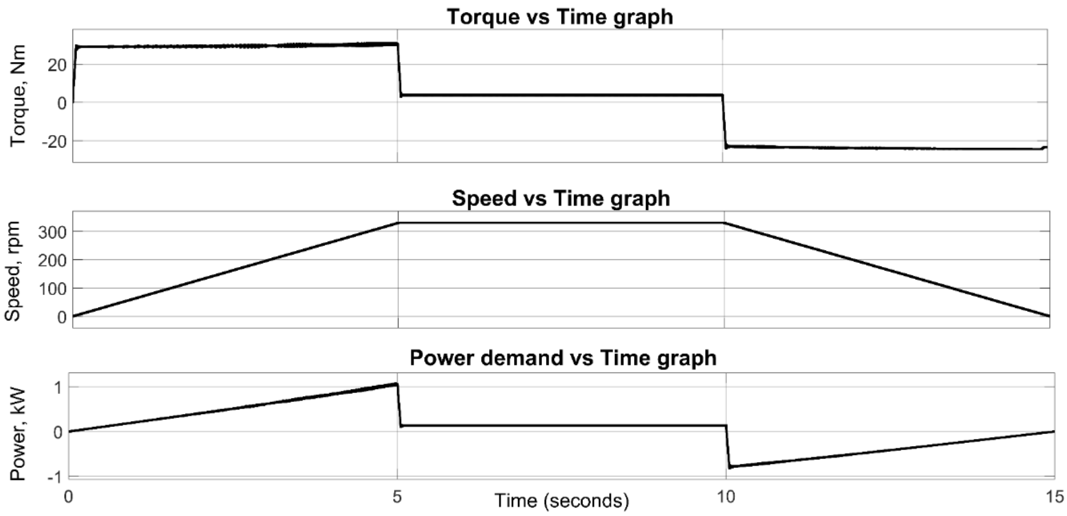

Figure 9. Torque, speed and power demand for Case 1

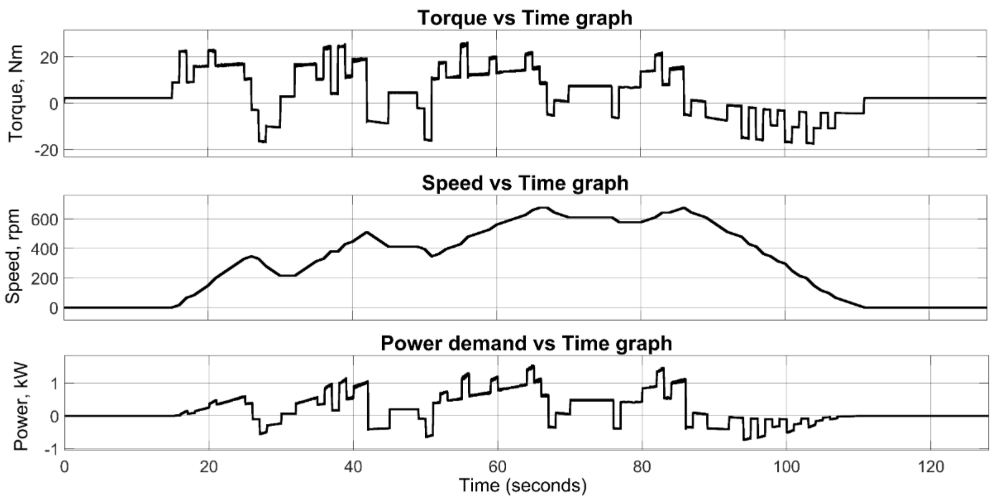

Figure 10. Torque, speed and power demand for Case 2

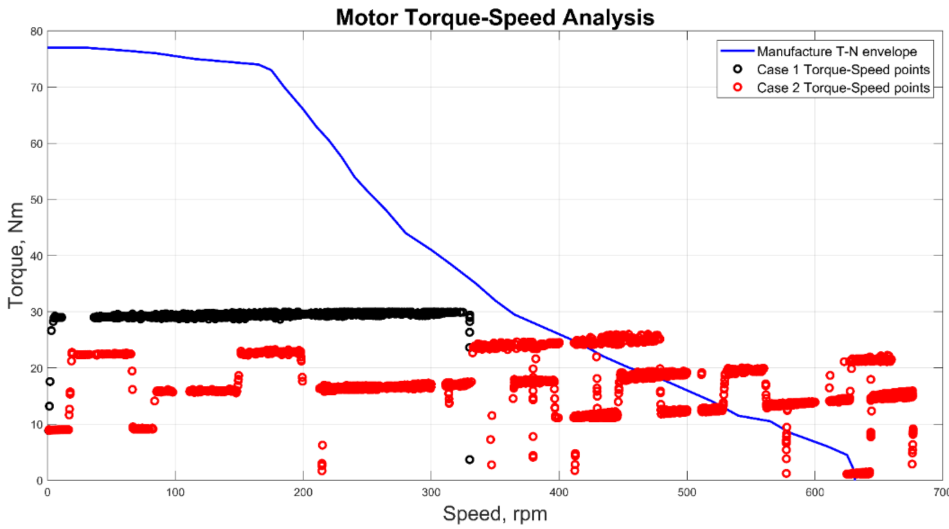

Figure 11. Distribution of operating points on Case 1 and 2 speed profiles

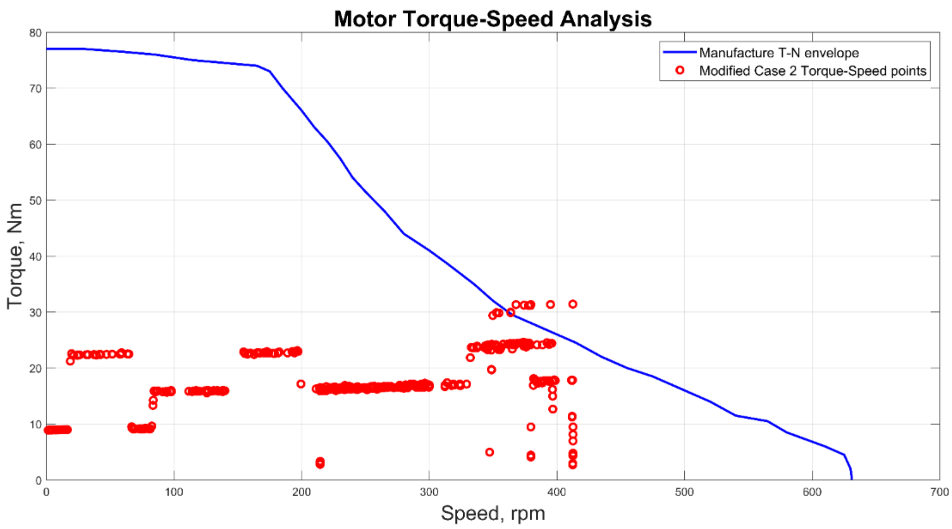

Figure 12. Distribution of operating points on modified Case 2 speed profile

5. CONCLUSION

This paper presents the modeling of a general PM BLDC motor designed to verify its performance under different speed profiles. The motor and longitudinal vehicle dynamics models were developed and analyzed in MATLAB software. The simulation results showed that the method could be used at the design stage of the PM BLDC motors in electric vehicle applications. The simulations would be more practical if the model had motor, controller, and transmission efficiency.

REFERENCES

[1] K. T. Chau, *Electric Vehicle Machines and Drives: Design, Analysis and Application*, John Wiley & Sons Singapore Pte. Ltd., 2015.

[2] M. Yildirim, M. Polat and H. Kurum, A survey on comparison of electric motor types and drives used for electric vehicles, *16th International Power Electronics and Motion Control Conference and Exposition*, Antalya, Turkey, 2014, 21-24.

[3] G. Luthra, Comparison of characteristics of various motor drives currently used in electric vehicle propulsion system, *International Journal of Mechanical and Production Engineering,* 5(6), 2017, 38-41.

[4] K. T. Chau, S. Member, C. C. Chan and C. Liu, Overview of permanent-magnet brushless drives for electric and hybrid electric vehicles, *IEEE Transactions on Industrial Electronics*, 55(6), 2008, 2246-2257.

[5] N. Ravi, S. Ekram and D. Mahajan, Design and development of an in-wheel brushless DC Motor drive for an electric scooter, *International Conference on Power Electronic, Drives and Energy Systems*, New Delhi, India, 2006.

[6] P. Gottipati, D. Oleksandr and E. A. Mendrela, In-wheel brushless DC Motor for a wheel chair drive, *Joint International Conference on Power Electronics, Drives and Energy Systems & 2010 Power India*, New Delhi, India, 2010.

[7] S. M. Lukic and A. Emado, Modeling of electric machines for automotive applications using efficiency maps, *Proceedings of Electrical Insulation Conference and Electrical Manufacturing and Coil Winding Technology Conference,* Indianapolis, USA, 2003.

[8] P. Lazari, J. Wang and L. Chen, A computationally efficient design technique for electric vehicle traction machines, *IEEE Transactions on Industry Applications*, 50(5), 2012, 3203-3213.

[9] S. K. Shet, Stability analysis of a novel PMBLDC motor drive for electric scooter application, *2015 Annual IEEE India Conference (INDICON),* New Delhi, India, 2015.

[10] C. Huang, F. Lei, X. Han and Z. Zhang, Determination of modeling parameters for a brushless DC Motor that satisfies the power performance of an electric vehicle, *Measurement and Control*, 52(7-8), 2019, 765-774.

[11] R. Krishnan, *Permanent Magnet Synchronous and Brushless DC Motor drives*. CRC Press/Taylor & Francis, 2010.

[12] C. L. Xia, *Permanent Magnet Brushless DC Motor Drives and Controls*, John Wiley & Sons, 2012.

[13] P. R. Babu, S. Ramprasath and B. Paranthagan, Modeling and dynamic simulation of permanent magnet brushless DC motor (PMBLDCM) drives, *Communications in Computer and Information Science*, 2013, 556-564.

[14] J. V. Mierlo, P. V. D. Bossche and G. Maggetto, Simulation methodologies for innovative vehicle drive systems, in *Finds and Results from the Swedish Cyprus Expedition: A Gender Perspective at the Medelhavsmuseet,* 2004.

[15] M. Ehsani, Y. Gao, S. E. Gay and A. Emadi, *Modern Electric, Hybrid Electric, and Fuel Cell Vehicles: Fundamentals, Theory, and Design*, CRC Press, 2004.

[16] Z. Song, X. B. Fan and J. Gan, Review on control of permanent magnet brushless DC Motor for electric vehicle, *International Journal of Electric and Hybrid Vehicles,* 10(4), 2018, 347-365.

[17] H. Wang, Design and implementation of brushless DC Motor drive and control system, *Procedia Engineering*, 29, 2012, 2219-2224.

[18] The Engineering Toolbox (Website), https://www.engineeringtoolbox.com/drag-coefficient-d_627.html, 2022 (accessed 20.08.2022).